

COMMUNICATIONS

Rydberg–London potential for diatomic molecules and unbonded atom pairs

Kevin Cahill^{a)}*Department of Physics and Astronomy, University of New Mexico, Albuquerque, New Mexico 87131 and Center for Molecular Modeling, Center for Information Technology, National Institutes of Health, Bethesda, Maryland 20892-5624*V. Adrian Parsegian^{b)}*National Institute of Child Health and Human Development, National Institutes of Health, Bethesda, Maryland 20892-0924*

(Received 13 September 2004; accepted 19 October 2004)

We propose and test a pair potential that is accurate at all relevant distances and simple enough for use in large-scale computer simulations. A combination of the Rydberg potential from spectroscopy and the London inverse-sixth-power energy, the proposed form fits spectroscopically determined potentials better than the Morse, Varnshi, and Hulburt–Hirschfelder potentials and much better than the Lennard-Jones and harmonic potentials. At long distances, it goes smoothly to the London force appropriate for gases and preserves van der Waals's "continuity of the gas and liquid states," which is routinely violated by coefficients assigned to the Lennard-Jones 6-12 form. © 2004 American Institute of Physics. [DOI: 10.1063/1.1830011]

There are at least three classes of interatomic potentials. Commercial codes use the Lennard-Jones

$$V_{LJ}(r) = |V(r_0)| \left[\left(\frac{r_0}{r} \right)^{12} - 2 \left(\frac{r_0}{r} \right)^6 \right] \quad (1)$$

and harmonic

$$V_H(r) = V(r_0) + \frac{(r-r_0)^2}{2} \frac{d^2V(r_0)}{dr^2} \quad (2)$$

forms, which are accurate near the minimum at $r=r_0$. But this first class of potentials may be too simple for complex materials away from equilibrium.

The Morse¹

$$V_M(r) = |V(r_0)| [(1 - e^{-\kappa x})^2 - 1] \quad (3)$$

($x = r - r_0$, $\kappa = \sqrt{k_e/(2|V(r_0)|)}$), Varnshi²

$$V_V(r) = |V(r_0)| \left[\left(1 - \frac{r_0}{r} e^{-\beta(r^2 - r_0^2)} \right)^2 - 1 \right] \quad (4)$$

($\beta = (\kappa r_0^2 - 1)/(2r_0^2)$), and Hulburt–Hirschfelder³

$$V_{HH}(r) = V_M(r) + |V(r_0)| c' \kappa^3 x^3 e^{-2\kappa x} (1 + \kappa b' x) \quad (5)$$

(for b' , c' , and k_e , see Ref. 4) potentials represent a second class of potentials⁴ accurate over a wider range of distances.

Quantum chemists^{5–9} have derived a third class that reproduce spectroscopic and thermodynamic data with impres-

sive fidelity. But the potentials of this class involve many parameters and may be too cumbersome for use in large-scale simulations.

We propose and test a form

$$V(r) = a e^{-br} (1 - cr) - \frac{d}{r^6 + e r^{-6}} \quad (6)$$

that is nearly as accurate as the class-3 potentials but simpler than many class-2 potentials. It is a combination of the Rydberg formula used in spectroscopy and the London formula for pairs of atoms. In Eq. (6), the terms involving a , b , and c were proposed by Rydberg¹⁰ to incorporate spectroscopic data, but were largely ignored until recently.^{11,12} The constant $d = C_6$ is the coefficient of the London tail. The new term $e r^{-6}$ cures the London singularity. As $r \rightarrow 0$, $V(r) \rightarrow a$, finite; as $r \rightarrow \infty$, $V(r)$ approaches the London term, $V(r) \rightarrow -d/r^6 = -C_6/r^6$. In a perturbative analysis,¹³ the a , b , c terms arise in first order, and the d term in second order.

To test whether the hybrid $V(r)$ can represent covalent bonds far from equilibrium, we used Gnuplot¹⁴ to fit Eq. (6) to empirical potentials for molecular H_2 , N_2 , and O_2 obtained from spectroscopic data^{15–17} by the RKR (Rydberg,¹⁰ Klein,¹⁸ Rees¹⁹) method, setting d equal to the London values. Figure 1 shows that the hybrid potential of Eq. (6) (solid, red) goes through the RKR points for H_2 (pluses, blue) from 0.5 to 4 Å. Fitted to the minimum, the harmonic potential (2) (dashes, green) and the Lennard-Jones potential (1) (dashes, blue) are accurate only near the minimum at 0.74 Å. Figure 2 shows that the hybrid potential $V(r)$ fits the O_2 RKR points.¹⁷ Figure 3 of our arXived paper²⁰ shows that the hybrid potential also fits the RKR points¹⁶ and the first-order

^{a)}Electronic mail: cahill@unm.edu

^{b)}Electronic mail: aparsegi@helix.nih.gov

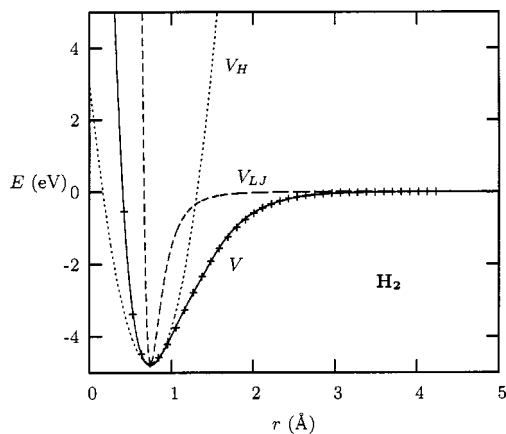


FIG. 1. The hybrid form V (with $a=53.8$ eV, $b=2.99$ Å⁻¹, $c=2.453$ Å⁻¹, $d=C_6=3.884$ eV Å⁶, and $e=47.6$ Å¹²) (solid, red) fits the RKR spectral points for the ground state of molecular hydrogen (pluses, blue) and gives the correct London tail for $r>3$ Å. The Lennard-Jones V_{LJ} (dashes, green) and harmonic V_H (dots, magenta) forms fit only near the minimum.

(FO) points²¹ for N₂ between 1 and 1.8 Å. The Lennard-Jones and harmonic potentials of Eqs. (1)–(2) fit only near the minima.

How does the hybrid form compare with the class-2 potentials of Eqs. (3)–(5)? Figures 3 and 4 (and Fig. 4 of Ref. 20) show that for $1.4 < r < 2$ Å the hybrid $V(r)$ is closer than (3)–(5) to the RKR points. A useful estimate of how well a particular potential $V_P(r)$ fits N data points $V_D(r_i)$ is the dimensionless error

$$\delta = \frac{1}{|V_D(r_0)|} \left[\frac{1}{N} \sum_{i=1}^N (V_P(r_i) - V_D(r_i))^2 \right]^{1/2}. \quad (7)$$

For H₂, N₂, and O₂, the average error δ was 59.7 for V_H , 49.3 for V_{LJ} , 0.037 for V_M , 0.031 for V_V , 0.021 for V_{HH} , and 0.0044 for the hybrid V . The hybrid form V is five times more accurate than the class-2 potentials (3)–(5) and four orders of magnitude more accurate than the class-1 potentials (1)–(2).

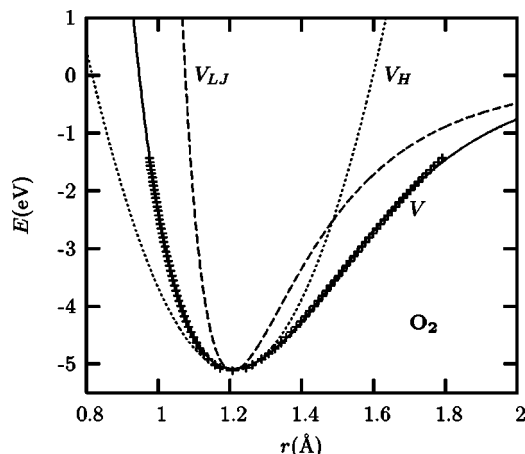


FIG. 2. For the ground state of molecular oxygen, the potential V of Eq. (6) (with $a=3.61$ keV, $b=4.48$ Å⁻¹, $c=1.05$ Å⁻¹, $d=16.08$ eV Å⁶, and $e=58.4$ Å¹²) (solid, red) fits the RKR points (pluses, blue). V_{LJ} and V_H as in Fig. 1.

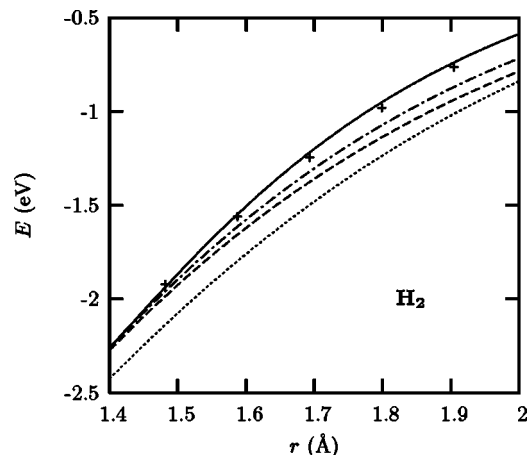


FIG. 3. The hybrid form V [Eq. (6) as in Fig. 1, solid, red] fits the RKR spectral points for the ground state of molecular hydrogen (pluses, blue). The Morse V_M [Eq. (3), dashes, green], Varnshi V_V [Eq. (4), dots, magenta], and Hulbert-Hirschfelder V_{HH} [Eq. (5), dot-dash, cyan] are too low for $1.5 < r < 3$ Å.

Can $V(r)$ also represent weak noncovalent bonds? Using Gnuplot, we fitted a , b , c , and e in Eq. (6) to Aziz's accurate HFDID1 potential for Ar₂ (Ref. 6) and HFD-B potential for Kr₂ (Ref. 22) and set d equal to their London-tail coefficients. Figures 5–8 show that for $2 \leq r \leq 7$ Å, the hybrid form (6) (solid, red) fits the Aziz potentials for both Ar₂ and for Kr₂ (pluses, blue). The Lennard-Jones V_{LJ} curves (1) (dashes, green) matched at the minima are too deep for $r > 4.5$ Å (Figs. 5 and 7) and too hard for $r < 3$ Å (Figs. 6 and 8). The potential $V(r)$ of Eq. (6) represents weak noncovalent bonds better than V_{LJ} (and V_H).

Does it matter that $V_{LJ}(r)$ fails to fit the Ar–Ar and Kr–Kr interactions? To find out, we used V and V_{LJ} to compute the dimensionless second virial coefficient B_2/r_0^3 of Ar and Kr at room temperature ($kT=0.025$ eV). Here r_0 is the minimum of the potential, and the second virial coefficient B_2 is the integral over all space

$$B_2(T) = -\frac{1}{2} \int d^3r (e^{-\beta V(r)} - 1) \quad (8)$$

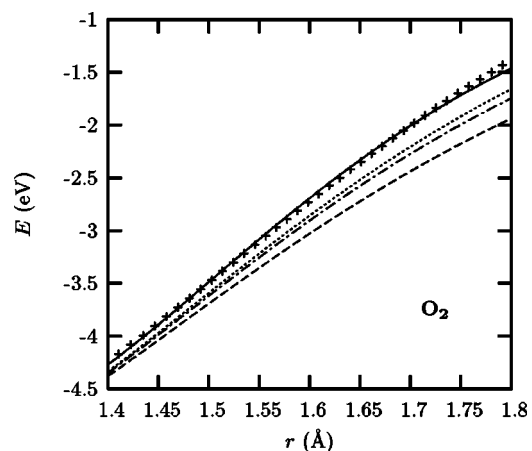


FIG. 4. For the ground state of molecular oxygen, the hybrid form V [Eq. (6), as in Fig. 3, solid, red] fits the RKR spectral points (pluses, blue). V_M , V_V , and V_{HH} as in Fig. 3.

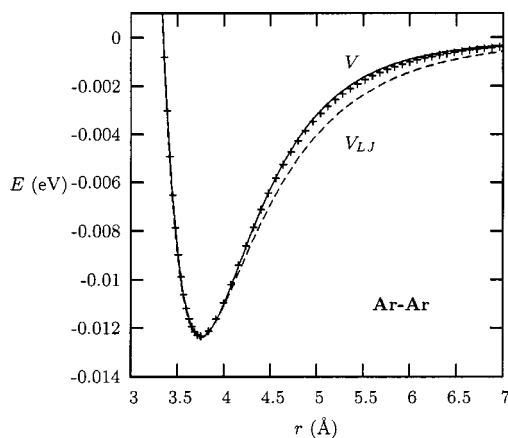


FIG. 5. The potential V [Eq. (6) for the Ar-Ar ground state with $a = 1720$ eV, $b = 2.6920 \text{ \AA}^{-1}$, $c = 0.2631 \text{ \AA}^{-1}$, $d = 37.943 \text{ eV \AA}^6$, and $e = 177588 \text{ \AA}^{12}$] (solid, red) fits the Ar₂ Aziz potential (pluses, blue) with the correct London tail. When matched at the minimum, the Lennard-Jones form V_{LJ} [Eq. (1) with $r_0 = 3.757 \text{ \AA}$ and $V(r_0) = -0.01234 \text{ eV}$] (dashes, green) is too low for $r > 4 \text{ \AA}$.

in which $\beta = 1/(kT)$. The hybrid potential V fitted to the curves of Figs. 5–8 gives $B_2/r_0^3 = -0.499$ for Ar and -1.35 for Kr, which respectively differ from the experimental²³ values of -0.552 and -1.41 by 9.6% and 4.1%. The Lennard-Jones potential V_{LJ} fitted to r_0 and $V(r_0)$ gives $B_2/r_0^3 = -0.899$ for Ar and -1.92 for Kr (errors of 63% and 37%); it also wags a long-range tail with a London coefficient $2|V(r_0)|r_0^6$ that is too large by 83% for Ar and by 84% for Kr. If the parameters r_0 and $V(r_0)$ in Eq. (1) for V_{LJ} are chosen to give the correct second virial coefficient B_2/r_0^3 for a range of temperatures,²⁴ then $V(r_0)$ is too shallow by 16% for Ar and 15% for Kr, and the London coefficients of the long-range tail are too large by 70% for Ar and by 64% for Kr. With only two parameters, Lennard-Jones fits are procrustean.

What about additivity?^{25–27} When three or more atoms interact, their potential energy is not the sum of the three (or more) pair potentials. Is the accuracy of the hybrid form important in the liquid phase where additivity is only approximate?

To test whether the lack of complete additivity in the

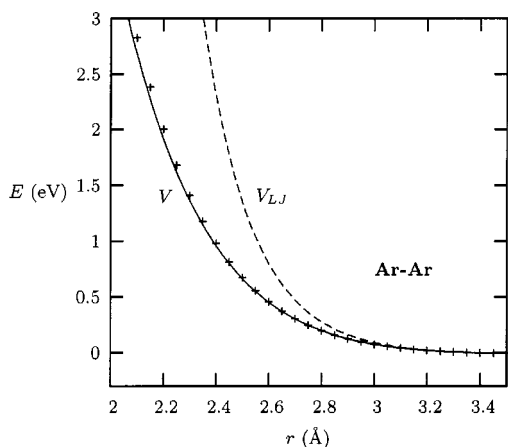


FIG. 6. Positive potential V [Eq. (6) as in Fig. 5], Ar₂ Aziz potential (pluses, blue), L-J form V_{LJ} [Eq. (1) as in Fig. 5].

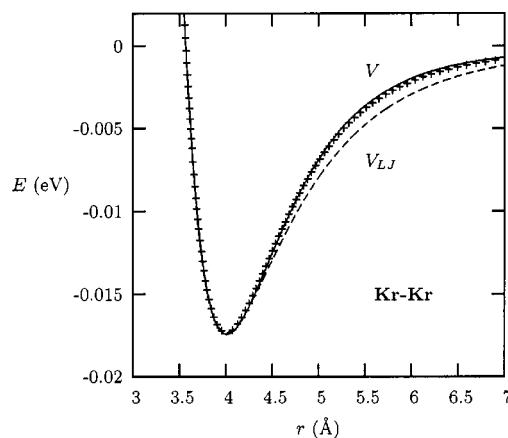


FIG. 7. The potential V [Eq. (6) for the Kr-Kr ground state with $a = 2499$ eV, $b = 2.5249 \text{ \AA}^{-1}$, $c = 0.2466 \text{ \AA}^{-1}$, $d = 78.214 \text{ eV \AA}^6$, and $e = 199064 \text{ \AA}^{12}$] (solid, red) fits the Kr₂ Aziz points (pluses, blue) with the correct London tail. When matched at the minimum, the Lennard-Jones form V_{LJ} [Eq. (1) with $r_0 = 4.008 \text{ \AA}$ and $V(r_0) = -0.017338 \text{ eV}$] (dashes, green) is too low for $r > 4 \text{ \AA}$.

liquid phase obscures the advantages of the hybrid form V over the Lennard-Jones potential V_{LJ} , we used both to compute the heats of vaporization $\Delta_{\text{vap}}H$ of Ar and Kr at their boiling points at atmospheric pressure. In our Monte Carlo simulations, we imposed periodic boundary conditions to reduce finite-size effects. Our Monte Carlo code is available at bio.phys.unm.edu/latentHeat. We used it to compute the potential energy U per atom in the liquid and gas phases. The latent heat of vaporization $\Delta_{\text{vap}}H$ is the difference between the potential energies U_{gas} and U_{liquid} plus the work done in expanding by ΔV against the pressure p of the atmosphere, $\Delta_{\text{vap}}H = U_{\text{gas}} - U_{\text{liquid}} + p\Delta V$.

The hybrid form V fitted to the curves of Figs. 5–8 gave $\Delta_{\text{vap}}H = 0.0694 \text{ eV}$ (per atom) for Ar and 0.0982 eV for Kr, which differ from the experimental values²³ of 0.0666 and 0.0941 eV by 4.2% and 4.4%. In equivalent Monte Carlo simulations, the Lennard-Jones potential V_{LJ} fitted to r_0 and $V(r_0)$ gave and $\Delta_{\text{vap}}H = 0.0787 \text{ eV}$ for Ar and 0.111 eV for Kr (errors of 18% and 18%). So the errors due to a lack of additivity are of the order of 4%, while those due to the Lennard-Jones potential are about 18%. Even in the liquid

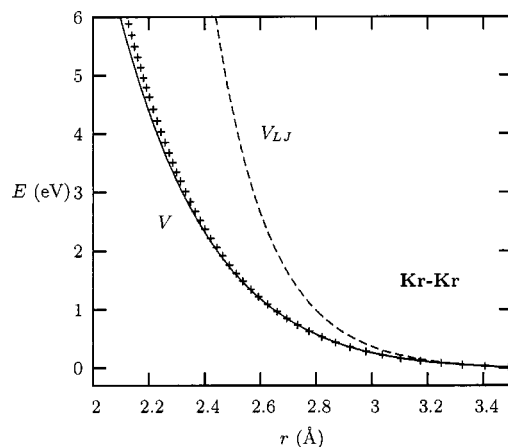


FIG. 8. Positive potential V [Eq. (6) as in Fig. 7], Kr₂ Aziz points (pluses, blue), L-J form V_{LJ} [Eq. (1) as in Fig. 7].

phase, limited additivity is less of a problem than the defects of the Lennard-Jones potential.

For a wide class of atom pairs, the hybrid form (6) can reliably represent the best spectroscopically determined potentials over all relevant distance scales. It also yields accurate second virial coefficients and heats of vaporization. Its simplicity recommends it as a teaching tool. Given the differences between it and the commonly used Lennard-Jones, harmonic, Morse, Varnshi, and Hulbert–Hirschfelder potentials, it would be worthwhile to further examine the consequences of these differences in Monte Carlo searches for low-energy states of biomolecules and in numerical simulations of phase transitions and reactions far from equilibrium.

Thanks to S. Valone for conversations and for RKR data; to S. Atlas, C. Beckel, B. Brooks, J. Cohen, K. Dill, D. Harries, G. Herling, M. Hodoscek, R. Pastor, R. Podgornik, W. Saslow, and C. Schwieters for advice. P. J. Steinbach kindly hosted K.C. at NIH, where we used the Biowulf computers.

¹P. M. Morse, *Phys. Rev.* **34**, 57 (1929).

²Y. P. Varnshi, *Rev. Mod. Phys.* **29**, 664 (1957).

³H. M. Hulbert and J. O. Hirschfelder, *J. Chem. Phys.* **35**, 1901(L) (1961).

⁴D. Steele, E. R. Lippincott, and J. T. Vanderslice, *Rev. Mod. Phys.* **34**, 239 (1962).

⁵C. Douketis, J. M. Hutson, B. J. Orr, and G. Scoles, *Mol. Phys.* **52**, 763 (1984).

⁶R. A. Aziz, *J. Chem. Phys.* **99**, 4518 (1993).

⁷A. K. Dham and W. J. Meath, *Mol. Phys.* **99**, 991 (2001).

⁸K. T. Tang and J. P. Toennies, *J. Chem. Phys.* **118**, 4976 (2003).

⁹L. P. Viegas, M. Cernei, A. Alijah, and A. J. C. Varandas, *J. Chem. Phys.* **120**, 253 (2004).

¹⁰R. Rydberg, *Z. Phys.* **73**, 376 (1931).

¹¹J. Ferrante, H. Schlosser, and J. R. Smith, *Phys. Rev. A* **43**, 3487 (1991).

¹²J. N. Murrell, S. Carter, S. C. Farantos, P. Huxley, and A. J. C. Varandas, *Molecular Potential Energy Functions* (Wiley, New York, 1984), p. 9.

¹³K. Cahill and V. A. Parsegian (2003), arxiv.org/q-bio.BM/0312005

¹⁴<http://www.gnuplot.info/>

¹⁵S. Weissman, J. T. Vanderslice, and R. Battino, *J. Chem. Phys.* **39**, 2226 (1963).

¹⁶A. Lofthus and P. H. Krupenie, *J. Phys. Chem. Ref. Data* **6**, 113 (1977).

¹⁷P. H. Krupenie, *J. Phys. Chem. Ref. Data* **1**, 423 (1972).

¹⁸O. Klein, *Z. Phys.* **76**, 226 (1932).

¹⁹A. L. G. Rees, *Proc. Phys. Soc. London* **59**, 998 (1947).

²⁰K. Cahill and V. A. Parsegian (2004), arxiv.org/q-bio.BM/0410018.

²¹W. C. Ermler, A. D. McLean, and R. S. Mulliken, *J. Phys. Chem.* **86**, 1305 (1982), col. 4, table V.

²²R. A. Aziz and M. J. Slaman, *Mol. Phys.* **58**, 679 (1986).

²³D. R. Lide and H. V. Kehiaian, *CRC Handbook of Thermophysical and Thermochemical Data* (CRC Press, Boca Raton, 1994), pp. 69–71.

²⁴T. L. Hill, *An Introduction to Statistical Thermodynamics* (Dover, New York, 1986), p. 484.

²⁵B. M. Axilrod and E. Teller, *J. Chem. Phys.* **11**, 299 (1943).

²⁶Y. Muto, *Phys.-Math. Soc. Jap.* **17**, 629 (1943).

²⁷E. Cheng and M. W. Cole, *Phys. Rev. B* **38**, 987 (1988).